# Renormalization group approach to two-dimensional Coulomb interacting Dirac fermions with random gauge potential

Oskar Vafek and Matthew J. Case

*National High Magnetic Field Laboratory and Department of Physics, Florida State University, Tallahassee, Florida 32306, USA*

We argue that massless Dirac particles in two spatial dimensions with $1/r$ Coulomb repulsion and quenched random gauge field are described by a manifold of fixed points which can be accessed perturbatively in disorder and interaction strength, thereby confirming and extending the results of Herbut, Juricic, and Vafek [arXiv:0707.4171 (unpublished)]. At small interaction and small randomness, there is an infrared stable fixed curve which merges with the strongly interacting infrared unstable line at a critical endpoint, along which the dynamical critical exponent $z=1$.

The properties of two-dimensional massless Dirac fermions have recently sprung back into focus, largely due to the experimental discovery of the quantum Hall effect in graphene,[1,2] the single layer graphite. Moreover, the ability to control the density of carriers by the electrical field effect allows experimental access to the rich physics of the neutrality point, where in the clean noninteracting picture, the conduction and the valence bands touch. It is well known[3] that, at the neutrality point, the exchange self-energy gives a logarithmic enhancement of the Fermi velocity $v_F \rightarrow v_F + (e^2/4\epsilon_d)\ln(\Lambda/k)$, where $k$ is a small wave vector near the nodal point[3] and $\epsilon_d$ is the dielectric constant of the medium. Physically, this effect is due to the lack of screening of the $1/r$ Coulomb interaction, an important consequence of which is the suppression of the single particle density of states $[N(E)]$ at low energies. This in turn leads to the suppression of the electronic contribution to the low temperature specific heat.[4]

This suppression of $N(E)$ may lure one into the (incorrect) conclusion that, at $T=0$, the Coulomb interactions turn the clean system into an electrical insulator. However, the vertex corrections contribute an *exactly* compensating enhancement of the conductivity,[5] making the system a *metal* with its residual conductivity asymptotically equal to the noninteracting value $\sigma_0 = (\pi/8)e^2/h$ per node.

In this work, we analyze the effects of the unscreened Coulomb interactions and the quenched random gauge disorder beyond leading order in the perturbative renormalization group (RG) of Ref. 5. Our principal findings, which support and extend those of Ref. 5, are twofold: first, in the clean case, there is an unstable fixed point at finite strength of Coulomb interactions characterized by the dimensionless ratio $\alpha = e^2/(\hbar\epsilon_d v_F)$ which represents a quantum critical point (QCP) separating the semimetal from an excitonic insulator; second, the interplay between Coulomb interactions and disorder induces a downward curvature of the fixed line,[6,5] causing it to end at the clean QCP (see Fig. 1).

In two dimensions, the Hamiltonian for Coulomb interacting massless Dirac fermions in the presence of a quenched random gauge field can be written as

$$\mathcal{H} = \mathcal{H}_0 + \mathcal{H}_{dis} + \hat{V}, \tag{1}$$

with the free part given by

$$\mathcal{H}_0 = \sum_{j=1}^{N} \int d^2\mathbf{r}\, v_F [\psi_j^\dagger(\mathbf{r})\mathbf{p}\cdot\sigma\psi_j(\mathbf{r})], \tag{2}$$

where the operator $\psi_j$ annihilates a two-component Dirac fermion, $\mathbf{p}=-i\nabla$, $\sigma_i$ is the $i$th Pauli matrix, and we have set $\hbar=k_B=1$ for convenience, unless otherwise stated. $N$ represents the number of fermion species; for single layer graphene, $N=4$. The disorder part of the Hamiltonian is

$$\mathcal{H}_{dis} = \sum_{j=1}^{N} \lambda_j v_F \int d^2\mathbf{r}[a_\mu(\mathbf{r})\psi_j^\dagger(\mathbf{r})\sigma_\mu\psi_j(\mathbf{r})], \tag{3}$$

where $\mu=1,2$ and the quenched random gauge field is assumed to be uncorrelated

$$\langle a_\mu(\mathbf{r})\rangle = 0, \quad \langle a_\mu(\mathbf{r})a_\nu(\mathbf{r}')\rangle = \Delta\delta_{\mu\nu}\delta(\mathbf{r}-\mathbf{r}'). \tag{4}$$

The charges $\lambda_j=(-1)^j$ vary in sign from node to node as dictated by the overall time reversal symmetry of the system. The Coulomb interaction between Dirac fermions is given by
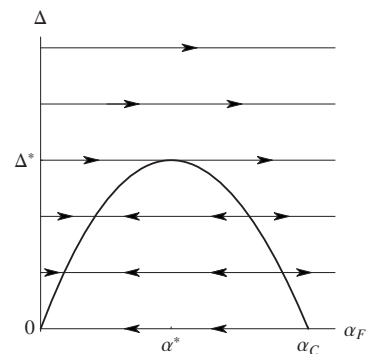


FIG. 1. The renormalization group flow diagram in the (disorder) $\Delta$-(interaction) $\alpha=e^2/(\epsilon_d v_F)$ plane. There is a line of stable fixed points at small $\Delta$ and small $\alpha$ which merges with the line of unstable fixed points at the critical end point. The (clean) unstable fixed point at $\alpha_c$ corresponds to a quantum phase transition into an excitonic insulator. Above the critical $\Delta^*$, the disordered but noninteracting fixed line is unstable directly to the insulator.
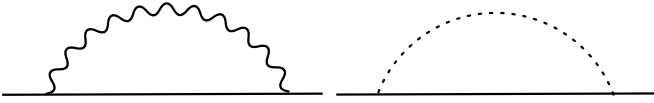
FIG. 2. Diagrams contributing to the self-energy to the first order in $\alpha_F$ and $\Delta_A$. As can be readily seen from the link cluster expansion, the second diagram comes with an overall sign.

$$\hat{V} = \frac{1}{2\epsilon_d} \int d^2\mathbf{r} d^2\mathbf{r}' \left[ \delta\hat{n}(\mathbf{r}) \frac{e^2}{|\mathbf{r} - \mathbf{r}'|} \delta\hat{n}(\mathbf{r}') \right], \quad (5)$$

where $\delta\hat{n}(\mathbf{r}) = \Sigma_j \psi_j^\dagger(\mathbf{r})\psi_j(\mathbf{r}) - n_0$ and $e$ is the electronic charge. The background charge density $n_0$ ensures overall charge neutrality.

This system can be described by three "coupling constants"—$e^2$, $\Delta$, and $v_F$—of which $\Delta$ is dimensionless and, in our units, both $v_F$ and $e^2/\epsilon_d$ have dimensions of velocity. In what follows, we will set $\epsilon_d = 1$ and restore it in the final results by rescaling the charge. Generically, these coupling constants flow under the renormalization group transformation. However, the charge $e^2$ does not flow because it is a coefficient on a nonanalytic term in the action, and as detailed elsewhere $\Delta$ does not flow either.[5] The entire flow of the renormalized coupling constants then comes from the scale dependence of the Fermi velocity. The RG beta functions take the form

$$\frac{de^2}{d \ln \kappa} = 0, \quad (6)$$

$$\frac{d\Delta}{d \ln \kappa} = 0, \quad (7)$$

$$\frac{dv_F}{d \ln \kappa} = v_F \frac{\Delta}{\pi} - \frac{e^2}{4} + \mathcal{A}v_F\Delta^2 + \mathcal{B}e^2\Delta + \mathcal{C}\frac{e^4}{v_F} + \cdots, \quad (8)$$

where the ellipses mean terms of cubic order in the double expansion in small $e^2$ and $\Delta$. The lowest order terms in the expansion come from the diagrams shown in Figs. 2–4.[5] The result of our analysis presented below is the following values of the above coefficients:

$$\mathcal{A} = 0, \quad \mathcal{B} = \frac{1}{8\pi}, \quad \mathcal{C} = \frac{N}{12} - \frac{103}{96} + \frac{3}{2} \ln 2. \quad (9)$$

The vanishing coefficient $\mathcal{A}$ agrees with the result of Ludwig *et al.*[7] that, for $e^2 = 0$, the dynamical critical exponent $z = 1 - d \ln v_F/d \ln \kappa = 1 - \Delta/\pi$ holds to all orders in perturbation
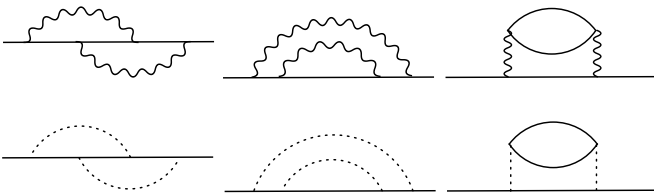


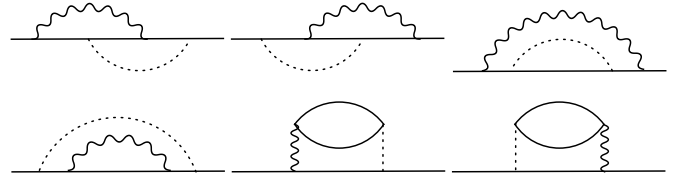FIG. 3. Diagrams contributing to the self-energy to the order $\alpha_F^2$ (first row) and $\Delta^2$ (second row).

theory. The values of $\mathcal{B}$ and $\mathcal{C}$ are the results reported in this paper.

If we rescale $e^2$ by $v_F$, we can define a dimensionless coupling constant $\alpha_F = e^2/(\hbar \epsilon_d v_F)$, which characterizes the strength of Coulomb interactions. The corresponding flow diagram is shown in Fig. 1. In the clean case, small $\alpha_F$ flows to zero due to the growth of the Fermi velocity. At $\alpha_F = \alpha_c$, there is a quantum phase transition into an excitonic insulator, controlled by the strongly interacting fixed point. Within the above approximation, for $N = 4$, which is appropriate for the single layer graphene, the unstable fixed point appears at $\alpha_c = 1/4\mathcal{C} \approx 0.833$. As discussed in greater detail below, since the expansion of the beta function (8) is carried out in $\alpha_F N \ll 1$, the semimetal-insulator fixed unstable point appears beyond the strict validity of the perturbative RG. Nevertheless, for finite $\Delta$, there is a fixed manifold given by

$$\Delta = \frac{\pi}{4} \frac{\alpha_F(1 - 4\mathcal{C}\alpha_F)}{1 + \pi\mathcal{B}\alpha_F}, \quad (10)$$

which is shown in Fig. 1 by the solid curve. Importantly, at small $\alpha_F$ and $\Delta$, this manifold represents the line of stable fixed points[6,5] which is asymptotically *exact*, and which merges with the line of unstable fixed points at the critical endpoint $(\alpha^*, \Delta^*)$.

Next, we detail the perturbative renormalization group calculation which we perform in dimensional regularization scheme by analytically continuing the space integrals to $D = 2 - \epsilon$ where $\epsilon > 0$. This formal device serves as a regulator for various divergent integrals. The bare Green's function has the form[8]

$$G_0(i\omega, \mathbf{k}) = (-i\omega + \sigma \cdot \mathbf{k})^{-1} = \frac{i\omega + \sigma \cdot \mathbf{k}}{\omega^2 + \mathbf{k}^2}.$$

The resulting self-energy matrix, which is defined through the two point irreducible vertex $\Gamma = \mathcal{G}^{-1}$ as

$$\Gamma_\mathbf{k}(i\omega) = -i\omega + v_F\sigma \cdot \mathbf{k} + \Sigma_\mathbf{k}(i\omega), \quad (11)$$

is calculated at finite external momentum $\mathbf{k}$ and frequency $i\omega$. To illustrate the procedure, consider the self-energy to first order in the coupling constant $e^2$ (the first diagram in Fig. 2):



FIG. 4. Diagrams contributing to the self-energy to the order $\alpha_F\Delta_A$.

$$\Sigma_{\mathbf{k}}^{exch}(i\omega) = 2\pi e^2 \int \frac{d^D\mathbf{q}}{(2\pi)^D} \int \frac{d\omega}{2\pi} \frac{1}{|\mathbf{k}-\mathbf{q}|} G_0(i\omega,\mathbf{q})$$

$$= e^2\sigma \cdot \mathbf{k} k^{D-2} \frac{\Gamma\left[1-\frac{D}{2}\right]\Gamma\left[\frac{D+1}{2}\right]\Gamma\left[\frac{D-1}{2}\right]}{(4\pi)^{D/2}\ \Gamma[D]}$$

$$\rightarrow e^2\sigma \cdot \mathbf{k} k^{-\epsilon}\left(\frac{1}{4\epsilon} + \frac{1}{8}\ln(64\pi e^{-\gamma_E})\right). \quad (12)$$

In the last line, we have used the analytic properties of the Euler $\Gamma$ functions and expanded the result near $\epsilon=0$. The Euler constant $\gamma_E \approx 0.577$. The pole at $D=2$ corresponds to a logarithmic divergence when a large momentum cutoff is introduced directly in two dimensions, i.e., the Hartree-Fock approximation leads to the logarithmic enhancement of velocity and $\Sigma_{\mathbf{k}}(i\omega) = \frac{e^2}{4}\sigma \cdot \mathbf{k} \ln \Lambda/k$ is frequency independent. This logarithmic enhancement of the Dirac velocity persists to second order in the coupling constant expansion, in qualitative agreement with Ref. 9, as well as the leading order expansion in large $N$.[10]

Similarly, the leading order self-energy due to the disorder scattering (second diagram in Fig. 2) is

$$\Sigma_{\mathbf{k}}^{dis}(i\omega) = \Delta \int \frac{d^D\mathbf{q}}{(2\pi)^D} \sigma_\mu G_0(i\omega,\mathbf{q})\sigma_\mu$$

$$= -\Delta i\omega|\omega|^{D-2}\frac{2\Gamma\left[1-\frac{D}{2}\right]}{(4\pi)^{D/2}}$$

$$\rightarrow -\Delta i\omega|\omega|^{-\epsilon}\left(\frac{1}{\pi\epsilon} + \frac{1}{2\pi}\ln(4\pi e^{-\gamma_E})\right). \quad (13)$$

Again, the pole at $D=2$ corresponds to a logarithmic divergence of the self-energy.

Before addressing the higher order contributions to the self-energy, let us define the renormalization conditions. The standard relationship between the renormalized two point function $\Gamma_{\mathbf{k}}^{ren}(i\omega)$ and the bare one (11) is

$$\Gamma_{\mathbf{k}}^{ren}(i\omega) = Z\Gamma_{\mathbf{k}}(i\omega), \quad (14)$$

where $Z$ is the wave-function renormalization.[11] The renormalized coupling constants can now be defined through the following renormalization conditions:

$$\frac{i}{2}\ \frac{\partial \text{Tr}[\Gamma_{\mathbf{k}}^{ren}(i\omega)]}{\partial\omega}\bigg|_{\omega=k=\kappa} = 1, \quad (15)$$

$$\frac{1}{4}\ \frac{\partial \text{Tr}[\sigma_\mu\Gamma_{\mathbf{k}}^{ren}(i\omega)]}{\partial k_\mu}\bigg|_{\omega=k=\kappa} = v_F^R. \quad (16)$$

Physically, the above equations demand that at the renormalization scale $\kappa$, the renormalized single particle Green's function $G_{\mathbf{k}}^{ren}(i\omega)$ takes the form

$$G_{\mathbf{k}}^{ren-1}(i\omega) = [-i\kappa + v_F^R\sigma \cdot \kappa]^{-1}.$$

From the above considerations, it is clear that, to find the RG flows, we need only to find the self-energies for $\omega=|\mathbf{k}|=\kappa$. At the orders $\Delta^2$, $e^2\Delta$, and $e^4$ we find

$$\Sigma^{(a)}(i\omega,\mathbf{k})\big|_\kappa = -i\omega\Delta^2\frac{\kappa^{-2\epsilon}}{2\pi^2}\left[\frac{1}{\epsilon^2} + \frac{\ln(4\pi e^{-\gamma_E})}{\epsilon}\right], \quad (17)$$

$$\Sigma^{(b)}(i\omega,\mathbf{k})\big|_\kappa = -i\omega\frac{e^2\Delta}{v_F}\frac{\kappa^{-2\epsilon}}{4\pi\epsilon} + \sigma \cdot \mathbf{k}e^2\Delta\kappa^{-2\epsilon}\left[\frac{1}{8\pi\epsilon^2}\right.$$

$$\left. + \frac{2\ln(16\pi e^{-\gamma_E})+3}{16\pi\epsilon}\right], \quad (18)$$

$$\Sigma^{(c)}(i\omega,\mathbf{k})\big|_\kappa = [-i\omega - v_F\sigma \cdot \mathbf{k}]\frac{e^4}{v_F^2}\frac{N}{4}\frac{\kappa^{-2\epsilon}}{12\epsilon} - i\omega\frac{e^4}{v_F^2}\frac{\kappa^{-2\epsilon}}{4\epsilon}\left[-\frac{2}{3}\right.$$

$$\left. + \ln 2\right] + \sigma \cdot \mathbf{k}\frac{e^4}{v_F}\frac{\kappa^{-2\epsilon}}{32\epsilon}\left[\frac{71}{6} - 16\ln 2\right]. \quad (19)$$

Thus, to this order in the perturbative expansion, the self-energy matrix in Eq. (11) is

$$\Sigma_{\mathbf{k}}(i\omega) = \Sigma_{\mathbf{k}}^{exch}(i\omega) + \Sigma_{\mathbf{k}}^{dis}(i\omega) + \Sigma_{\mathbf{k}}^a(i\omega) + \Sigma_{\mathbf{k}}^b(i\omega) + \Sigma_{\mathbf{k}}^c(i\omega),$$

and using Eqs. (14)–(16) we find the RG flow equation for the renormalized Fermi velocity to be

$$\frac{dv_F^R}{d\ln\kappa} = -\frac{e^2}{4} + v_F^R\frac{\Delta}{\pi} + \frac{e^2\Delta}{8\pi} + \left(\frac{N}{12} - \frac{103}{96} + \frac{3}{2}\ln 2\right)\frac{e^4}{v_F^R}.$$

This is the result displayed in Eq. (8). It is apparent from this flow equation that at $\Delta=0$ the Fermi velocity increases logarithmically provided that the dimensionless coupling $\alpha < \alpha_c$. Such logarithmic growth implies suppression of the electronic density of states near the Dirac point and concomitant suppression of the specific heat.[4]

In the case of $\alpha > \alpha_c$, the runaway RG flows can be interpreted as the flow toward an excitonic insulator. The physical nature of this insulator depends on the details of the lattice model. For spinless fermions on a honeycomb lattice, for example, it would correspond to a state with a spontaneous breaking of (plaquette or bond centered) inversion symmetry and unequal population of the two sublattices; for strictly $1/r$ Coulomb repulsion and for the spinfull case, it would correspond to an "antiferromagnetic" order (but no unit cell doubling) with unequal spin population of the two sublattices, although details of the short range part of the repulsive in-
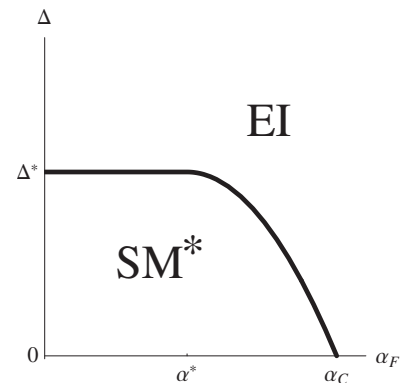


FIG. 5. Phase diagram in the interaction-disorder plane as determined from Fig. 1. The solid line separates the disordered semimetallic phase (SM*) from the excitonic insulator (EI).

teractions could destabilize it toward the inversion symmetry broken state with unequal charge population of the two sublattices.[12]

We conclude with a discussion of the validity of the approximations employed here. First, the RG was organized perturbatively in both $\alpha$ and $\Delta$ so the weak coupling portion of the fixed line in Fig. 1 is rigorously justified. Additionally, the downward curvature of this line implied by the sign of the terms in the second order expansion is also rigorous. Diagrammatically, integration of these RG equations corresponds to an infinite parquetlike resummation of the two leading logarithms at each order in the perturbative expansion (see, for instance, Ref. 13).

On the other hand, the unstable portion of the fixed line and the (unstable) clean fixed point appear at a finite value of the coupling constant at which $\alpha_F N$ is not small. They are, therefore, beyond the reach of the perturbative RG. Nevertheless, the very *existence* of the clean unstable fixed point is perhaps on somewhat firmer footing,[14–16] and due to the negative curvature of the IR stable fixed line in the perturbatively accessible region of the flow diagram, we expect that the gross topological features of the fixed manifold in Fig. 1 and the phase diagram in Fig. 5, if not their quantitative aspects, are valid.

[1] K. S. Novoselov, A. K. Geim, S. V. Morozov, D. Jiang, M. I. Katsnelson, I. V. Grigorieva, S. V. Dubonos, and A. A. Firsov, Nature (London) **438**, 197 (2005).

[2] Y. Zhang, Y.-W. Tan, H. L. Stormer, and P. Kim, Nature (London) **438**, 201 (2005).

[3] J. Gonzales, F. Guinea, and M. A. H. Vozmediano, Nucl. Phys. B **424**, 595 (1994).

[4] O. Vafek, Phys. Rev. Lett. **98**, 216401 (2007).

[5] I. F. Herbut, V. Juricic, and O. Vafek, arXiv:0707.4171 (unpublished).

[6] T. Stauber, F. Guinea, and M. A. H. Vozmediano, Phys. Rev. B **71**, 041406 (2005).

[7] A. W. W. Ludwig, M. P. A. Fisher, R. Shankar, and G. Grinstein, Phys. Rev. B **50**, 7526 (1994).

[8] J. W. Negele and H. Orland, *Quantum Many-Particle Systems* (Addison-Wesley, Reading, MA, 1988).

[9] E. G. Mishchenko, Phys. Rev. Lett. **98**, 216801 (2007).

[10] J. González, F. Guinea, and M. A. H. Vozmediano, Phys. Rev. B **59**, R2474 (1999).

[11] M. E. Peskin and D. V. Schroeder, *An Introduction to Quantum Field Theory* (Addison-Wesley, Reading, MA, 1995).

[12] I. F. Herbut, Phys. Rev. Lett. **97**, 146401 (2006).

[13] I. F. Herbut, *A Modern Approach to Critical Phenomena* (Cambridge University Press, Cambridge, 2007).

[14] D. V. Khveshchenko, Phys. Rev. Lett. **87**, 246802 (2001).

[15] E. V. Gorbar, V. P. Gusynin, V. A. Miransky, and I. A. Shovkovy, Phys. Rev. B **66**, 045108 (2002).

[16] H. Leal and D. V. Khveshchenko, Nucl. Phys. B **687**, 323 (2004).